Supplementary Materials for

Unexpected strong paramagnetism of hydrogels containing carbon-oxygen double bonds induced by calcium cations

Ruoyang Chen, Yue-Yu Zhang, Xing Huang, Liping Wang, Lei Zhang, Chao Song, Lixiong Dai, Min Zhang, Jun Wang, Yong Jian, Weiyuan Xu, Hui Dong, Bingquan Peng, Shuqiang He, Shanshan Liang, Fangfang Dai, Qihui Fan, Fangfu Ye, Xin Zhang, Feng Zhang, Haiping Fang

Correspondence to: Haiping Fang, fanghaiping@sinap.ac.cn; Fangfu Ye, fye@iphy.ac.cn; Xing Zhang, xinzhang@hmfl.ac.cn; Feng Zhang, fzhang@usst.edu.cn

This PDF file includes:

1. Supplementary Figs. 1 to 9
2. Supplementary Tables 1 to 2
3. Supplementary Video captions 1 to 2

Other Supplementary Materials for this manuscript include the following:

Supplementary Videos 1 to 2

1. Supplementary Figs. 1 to 9

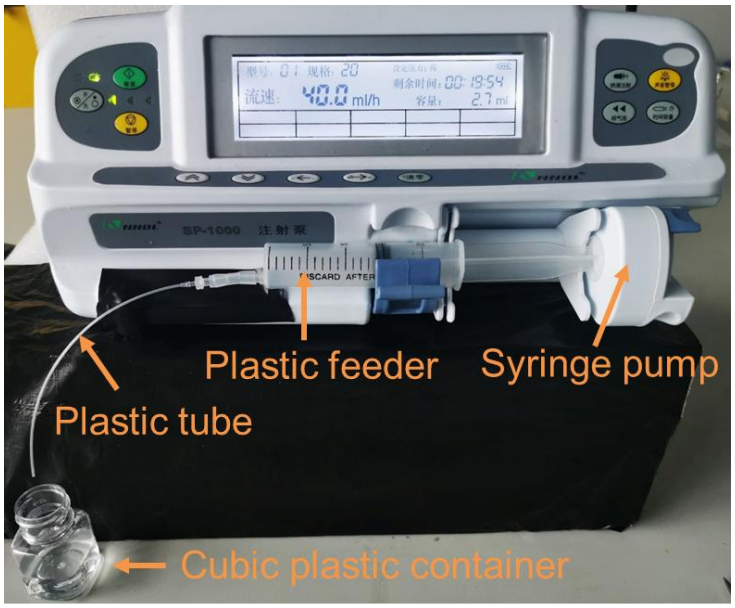

Supplementary Fig. 1. Custom-built plastic injection system for preparing the very strong paramagnetic Alg-Ca hydrogel. An automatic syringe pump was set to control the injection rate of the solution, an ultraclean plastic feeder was connected with a plastic tube for controlling the size of the injected solution drop, and a cubic plastic container was placed to collect the solution.

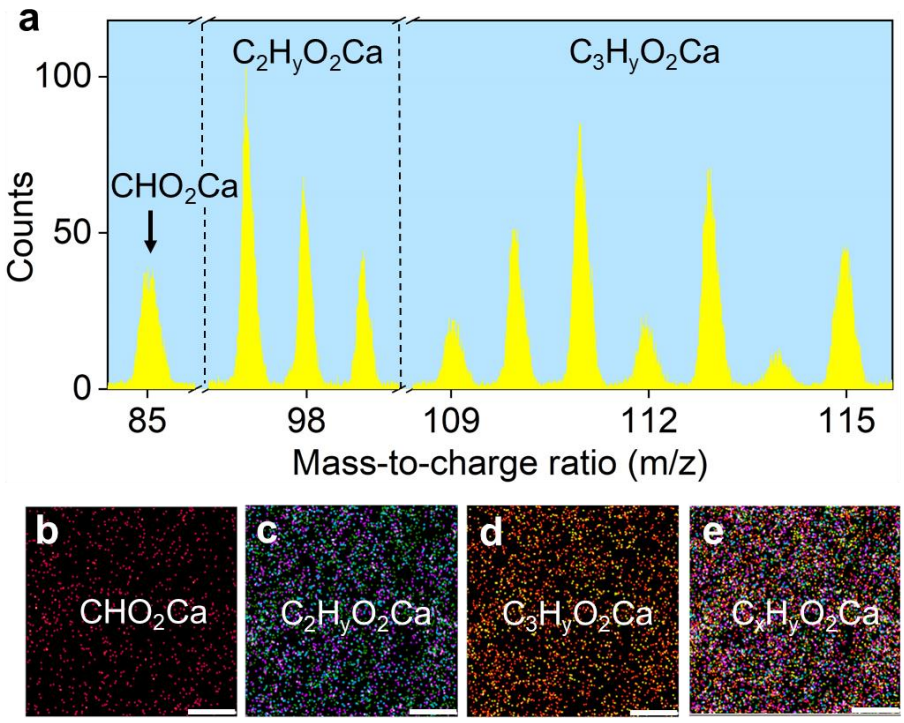

Supplementary Fig. 2. Structural analysis on the strong paramagnetic Alg-Ca hydrogel. (**a**) Time-of-flight secondary ion mass spectrum (ToF-SIMS) of the Alg-Ca hydrogel, clearly showing the characteristic peaks of $C_xH_yO_2Ca$. (**b**)-(**e**) Mapping distributions of corresponding charged fragments of CHO_2Ca, $C_2H_yO_2Ca$, $C_3H_yO_2Ca$, and $C_xH_yO_2Ca$ (merged by formers) in positive mode; scale bar: 20 μm.

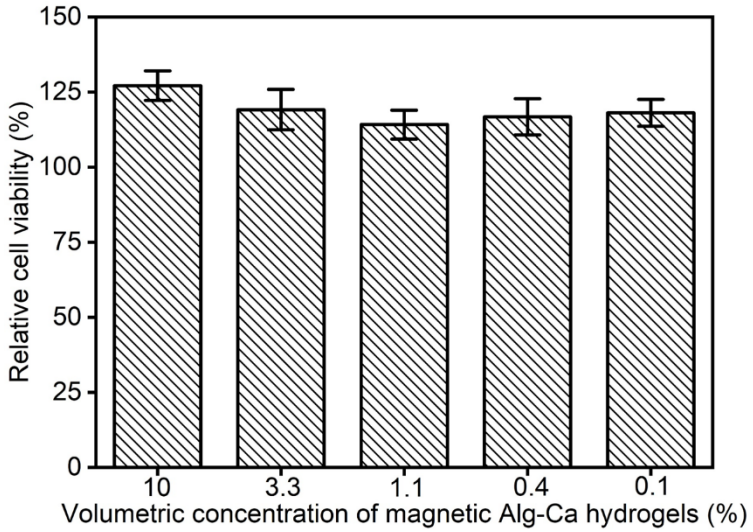

Supplementary Fig. 3. *In vitro* biocompatibility study of the Alg-Ca hydrogel. Relative cell viability of NIH-3T3 cells cultured with the medium containing different concentrations of the Alg-Ca hydrogel, showing that the Alg-Ca hydrogel has very low cytotoxicity.

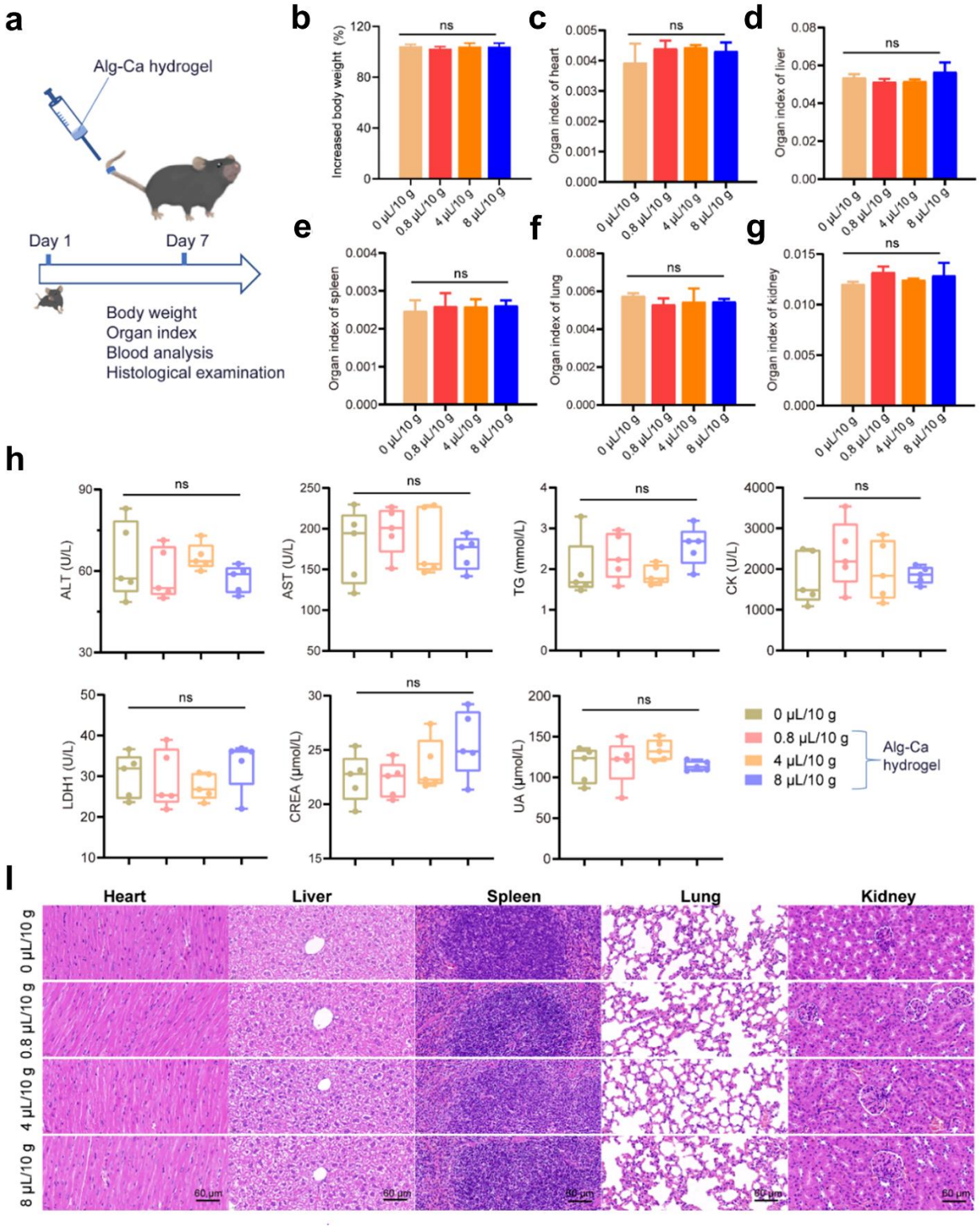

Supplementary Fig. 4. *In vivo* biocompatibility study of the Alg-Ca hydrogel. (**a**) Schematic illustration of the mouse models for safety evaluation. The C57B6/J healthy

mice were injected with saline or the Alg-Ca hydrogel intravenously at 0.8, 4 or 8 μL/10 g. Their body weight was monitored for a week before final examinations. (**b**) The increased body weight of mice. (**c-g**) The organ index of heart, liver, spleen, lung and kidney. (**h**) Serum alanine aminotransferase (ALT), aspartate aminotransferase (AST), triglycerides (TG), creatine kinase (CK), urea (UA), lactic dehydrogenase 1 (LDH1) and creatinine (CREA). (**i**) Hematoxylin & eosin staining of heart, liver, spleen, lung and kidney. Scale bar: 60 μm.

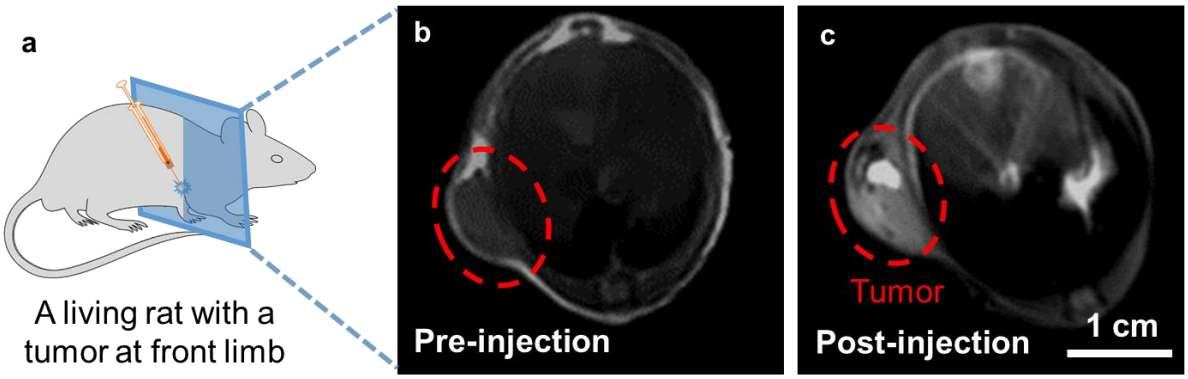

Supplementary Fig. 5. The Alg-Ca hydrogel applied for *in vivo* magnetic resonance imaging (MRI). (**a**) The paramagnetic Alg-Ca hydrogel was injected into a living Sprague-Dawley rat with a tumor at the front limb, followed by the MRI measurement. (**b**) and (**c**) Monochromatic MR images of a tumor (red dashed circle) in the rat before and after hydrogel injection.

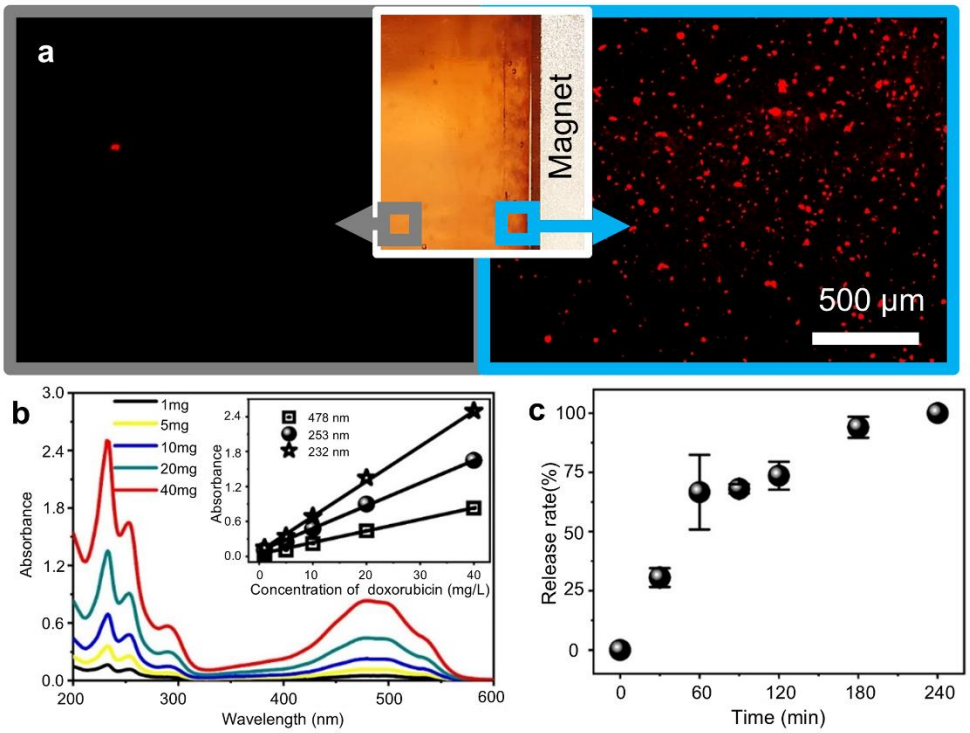

Supplementary Fig. 6. Drug release of the Dox@Alg-Ca hydrogel. (**a**) Fluorescent images of the hydrogel suspension extracted from areas far from (left) and close to (right) the magnet; red dots are the Dox@Alg-Ca hydrogel; inset in the middle shows that the Dox@Alg-Ca hydrogel is attracted towards the magnet; (**b**) UV-Vis spectra of the Dox in different concentrations; inset shows the linear fitting of the adsorption intensity versus the concentration of the Dox; (**c**) Concentration of the Dox released from the Dox@Alg-Ca hydrogel.

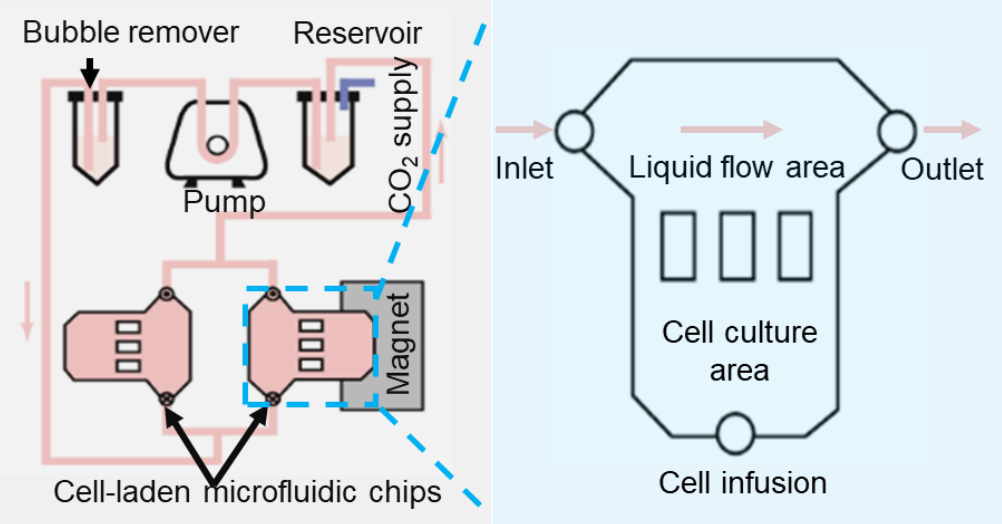

Supplementary Fig. 7. **Schematic illustration of the simulated human circulatory system**. A pump is designed as a power source for the liquid circulatory and is connected with two cell-laden microfluidic chips with and without a magnet underneath, respectively. The right image shows the cell-laden microfluidic chip with a liquid flow area and a cell culture area.

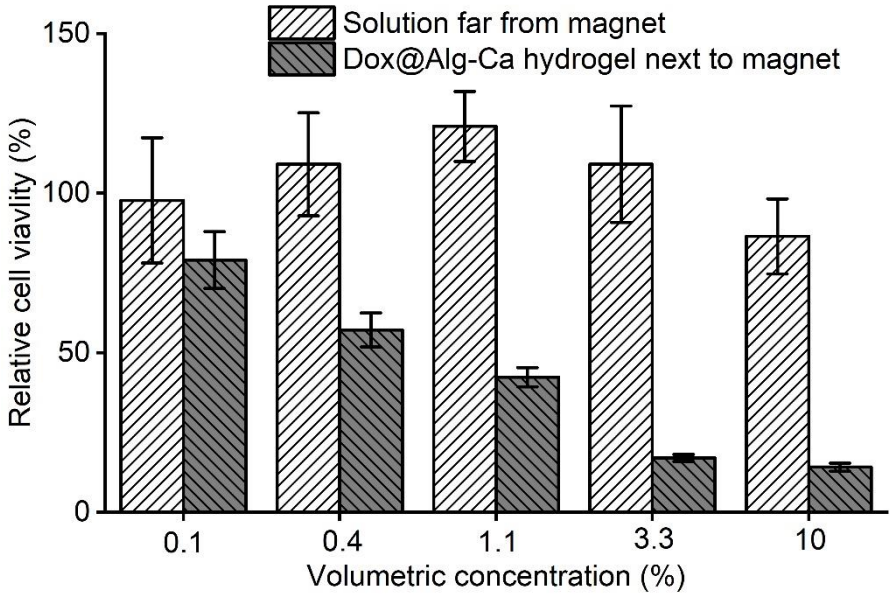

Supplementary Fig. 8. Effect of Dox@Alg-Ca hydrogel on the growth of A549 cells.

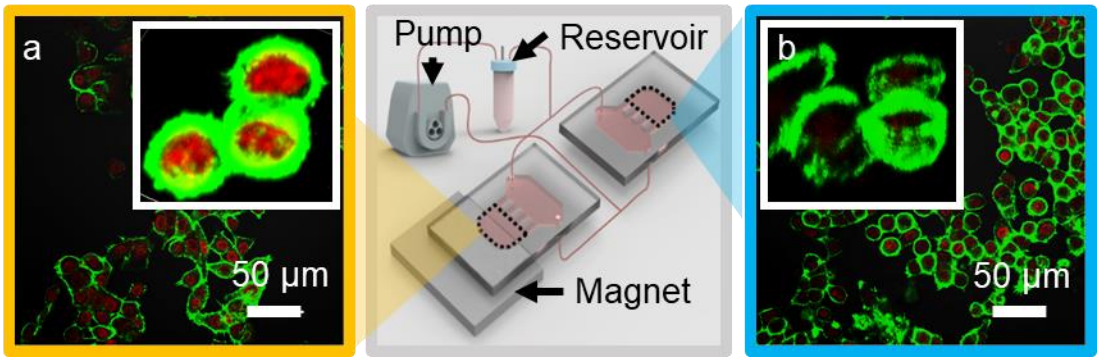

Supplementary Fig. 9. Drug uptake into A549 cells in the simulated human circulatory system. (**a**) Cells cultured in the area with a magnet; green represents the f-actin of cells stained by the FITC-phalloidin and red represents the Dox released from the Dox@Alg-Ca hydrogel; (**b**) Cells cultured in the area without magnet. The inserts show the enlarged images of the cells in these two regions.

2. Supplementary Tables 1 to 2

Supplementary Table 1. ICP-MS test of the Alg-Ca hydrogel

	The Alg-Ca hydrogel (ppb)			
Fe	9.3	9.3	6.4	8.4
Co	N/A	N/A	N/A	N/A
Ni	0.2	0.1	0.1	0.1
Mn	0.1	N/A	0.1	0.1
V	N/A	N/A	N/A	N/A
Cd	0.1	N/A	N/A	0.1
Cr	0.8	0.9	0.5	0.6
Gd	0.2	0.2	0.1	0.2
Nd	N/A	N/A	N/A	N/A
La	0.1	0.1	0.1	0.1
Mo	0.4	0.5	0.2	0.2
Ce	0.2	0.2	0.3	0.5
Pr	N/A	N/A	N/A	N/A
Sm	0.1	0.1	0.1	0.1
Eu	0.1	N/A	N/A	N/A
Dy	0.1	0.1	0.1	0.1
Ho	N/A	N/A	N/A	N/A
Tm	N/A	N/A	N/A	N/A
Yb	N/A	N/A	N/A	N/A
Er	N/A	N/A	N/A	N/A

Supplementary Table 2. EDX analysis of the AlgNa and strongly paramagnetic Alg-Ca hydrogel

	AlgNa		Alg-Ca hydrogel	
	Conc (wt.%)	Atomic%	Conc (wt.%)	Atomic%
C	30.542	39.074	23.553	32.219
O	51.243	49.215	58.127	59.693
Na	16.449	10.995	1.616	1.155
Cl	0.787	0.341	1.595	0.739
Ca	0.978	0.375	15.109	6.194
Total	100	100	100	100

3. Supplementary Video captions

Supplementary Video 1: In vivo magnetic resonance imaging (MRI) for a living Sprague-Dawley (SD) rat with a tumor at the front limb.

Supplementary Video 2: The paramagnetic Alg-Ca hydrogel applied for in vivo MRI for the tumor on the living SD rat.